

Forecasting range shifts of a dioecious plant species under climate change

Jacob K. Moutouama ^{*1}, Aldo Compagnoni², and Tom E.X. Miller¹

¹Program in Ecology and Evolutionary
Biology, Department of BioSciences, Rice University, Houston, TX USA

²Institute
of Biology, Martin Luther University Halle-Wittenberg, Halle, Germany; and
German Centre for Integrative Biodiversity Research (iDiv), Leipzig, Germany

Running header: Forecasting range shifts

Keywords: climate change, demography, forecasting, matrix projection model, mechanistic models, sex ratio, range limits

Acknowledgements: This research was supported by XX.

Authorship statement: XXXXX.

Data accessibility statement: All data (Miller and Compagnoni, 2022a) used in this paper are publicly available. Should the paper be accepted, all computer scripts supporting the results will be archived in a Zenodo package, with the DOI included at the end of the article. During peer review, our data and code are available at <https://github.com/jmoutouama/POAR-Forecasting>.

Conflict of interest statement: None.

^{*}Corresponding author: jmoutouama@gmail.com

1 Abstract

2 Rising temperatures and extreme drought events associated with global climate change have
3 triggered an urgent need for predicting species response to climate change. Currently, the
4 vast majority of theory and models in population biology, including those used to forecast
5 biodiversity responses to climate change, ignore the complication of sex structure. To address
6 this issue, we developed a climate-driven population matrix model using demographic data of
7 dioecious species (Texas bluegrass), past and future climate (different gas emission scenarios)
8 to forecast and backcast the effect of climate change on range shifts. Our results show a sex
9 specific demographic response to climate change. Female individuals have a demographic
10 advantage (higher vital rate) over males. Female demographic advantage led to a slight decline
11 in population viability under future climate assuming moderate gas emission and a drastic
12 reduction in population viability under future climate assuming high gas emission. Despite
13 a change in species range, climate change will likely alter population viability in dioecious
14 species. Overall, our work suggest that tracking only the female could lead to a slight overesti-
15 mation of the impact of climate change on dioecious species. This study provides a framework
16 for predicting the impact of climate on dioecious species using population demography.

¹⁷ Introduction

¹⁸ Rising temperatures and extreme drought events associated with global climate change are
¹⁹ leading to increased concern about how species will become redistributed across the globe
²⁰ under future climate conditions (Bertrand et al., 2011; Gamelon et al., 2017; Smith et al., 2024).
²¹ Dioecious species (most animals and many plants) might be particularly vulnerable to the
²² influence of climate change because they often display skewed sex ratios that are generated or
²³ reinforced by sexual niche differentiation (distinct responses of females and males to shared cli-
²⁴ mate drivers) (Tognetti, 2012). Accounting for such a niche differentiation within a population
²⁵ is a long-standing challenge in accurately predicting which sex will successfully track envi-
²⁶ ronmental change and how this will impact population viability and range shifts (Gissi et al.,
²⁷ 2023a; Jones et al., 1999). The vast majority of theory and models in population biology, includ-
²⁸ ing those used to forecast biodiversity responses to climate change, ignore the complication of
²⁹ sex structure (Ellis et al., 2017; Pottier et al., 2021). As a result, accurate forecasts of colonization-
³⁰ extinction dynamics for dioecious species under future climate scenarios are limited.

³¹ Climate change can influence dioecious populations via shifts in sex ratio.¹ Females and
³² males may respond differently to climate change, especially in species where there is sexual
³³ niche differentiation (Gissi et al., 2023a,b; Hultine et al., 2016). This sex-specific response to
³⁴ climate change may help one sex to succeed in extreme climatic conditions rather than the
³⁵ other sex (Bürli et al., 2022; Zhao et al., 2012) leading to a skewness in the operational sex ratio
³⁶ (relative number of males and females as available mates) (Eberhart-Phillips et al., 2017). For
³⁷ example, experiments in two populations of Atlantic marine copepods (*Acartia tonsa*) revealed
³⁸ that male survival was more sensitive to increasing temperatures than female survival (Sasaki
³⁹ et al., 2019). In other species, such as *Pteropus poliocephalus* or *Populus cathayana*, females
⁴⁰ showed lower survival than males in response to high temperature (Welbergen et al., 2008;
⁴¹ Zhao et al., 2012). Sex-specific responses to climate drivers have the potential to influence
⁴² population viability under global change because skew in the operational sex ratio can limit
⁴³ reproduction through mate scarcity (Petry et al., 2016).

⁴⁴ Species's range limits, when not driven by dispersal limitation, should generally reflect
⁴⁵ the limits of the ecological niche (Lee-Yaw et al., 2016). For most species, niches and geographic
⁴⁶ ranges are often limited by climatic factors including temperature and precipitation (Sexton
⁴⁷ et al., 2009). Therefore, any substantial changes in the magnitude of these climatic factors in a
⁴⁸ given location across the range could impact population viability, with implications for range
⁴⁹ shifts based on which regions become more or less suitable (Davis and Shaw, 2001; Pease

¹This paragraph is really good but notice that the topic sentence (and much that follows) is largely redundant with the first paragraph. I would suggest creating clearer distinction between paragraphs.

50 et al., 1989). Forecasting range shifts for dioecious species is complicated by the potential for
51 each sex to respond differently to climate variation (Morrison et al., 2016; Pottier et al., 2021).
52 Populations in which males are rare under current climatic conditions could experience low
53 reproductive success due to sperm or pollen limitation that may lead to population decline in
54 response to climate change that disproportionately favors females (Eberhart-Phillips et al., 2017).
55 In contrast, climate change could expand male habitat suitability (e.g. upslope movement),
56 which might increase seed set for pollen-limited females and favor range expansion (Petry
57 et al., 2016). Although the response of species to climate warming is an urgent and active area
58 of research, few studies have disentangled the interaction between sex and climate drivers
59 to understand their combined effects on population dynamics and range shifts.

60 Our ability to track the impact of climate change on the population dynamics of
61 dioecious plants and the implication of such impact on range shift depends on our ability
62 to build mechanistic models that take into account the spatial and temporal context in which
63 sex specific response to climate change affects population viability (Czachura and Miller, 2020;
64 Davis and Shaw, 2001; Evans et al., 2016). For example, structured models that are built from
65 long-term demographic data collected from common garden experiments have emerged as
66 powerful technic to study the impact of climate change on species range shift (Merow et al.,
67 2017; Schwinning et al., 2022). These structured models are increasingly utilized for two
68 reasons. First, they enable the manipulation of treatments that can isolate spatial and temporal
69 correlations between environmental factors, thus overcoming a main disadvantage with many
70 types of correlative studies (Leicht-Young et al., 2007). Second, they link individual-level
71 demographic trait to population demography allowing the investigation of the demographic
72 mechanisms behind vital rates (e.g. survival, fertility, growth and seed germination) response
73 environmental variation (Dahlgren et al., 2016; Louthan et al., 2022). Third, these structured
74 models can be used to identify which aspect of climate is more important for population
75 dynamics. For example, Life Table Response Experiment (LTRE) build from structured
76 models is an approach that has become widely used to understand how a given treatment
77 (eg. temperature or precipitation) could affect population dynamics (Caswell, 1989; Iler et al.,
78 2019; Morrison and Hik, 2007; O'Connell et al., 2024).

79 In this study, we used a mechanistic approach by combining geographically-distributed
80 field experiments, hierarchical statistical modeling, and two-sex population projection
81 modeling to understand the demographic response of dioecious species to climate change and
82 its implications for future range dynamics. Our study system is a dioecious plant species (*Poa*
83 *arachnifera*) distributed along environmental gradients in the south-central US corresponding
84 to variation in temperature across latitude and precipitation across longitude. A previous
85 study on the same system showed that, despite a differentiation of climatic niche between

86 sexes, the female niche mattered the most in driving the environmental limits of population
87 viability (Miller and Compagnoni, 2022b). However that study did not use climate variables
88 preventing us from backcasting and forecasting the impact of climate change on dioecious
89 species. Here, we asked four questions:

- 90 1. What are the sex-specific vital rate responses to variation in temperature and precipitation
91 across the species' range?
- 92 2. How sex-specific vital rates combine to determine the influence of climate variation on
93 population viability (λ)?
- 94 3. What are the historical and projected changes in climate across the species range?
- 95 4. What are the back-casted and fore-casted dynamics of this species' geographic niche
96 ($\lambda \geq 1$) and how does accountind for sex structure modify these predictions?

97 Materials and methods

98 Study species

99 Texas bluegrass (*Poa arachnifera*) is a dioecious perennial, summer-dormant cool-season (C3)
100 grass that occurs in the south-central U.S.(Texas, Oklahoma, and southern Kansas) (Hitchcock,
101 1971). Average temperatures along the distribution of the species tend to decrease northward
102 as a result of the influence of latitude: lower latitudes receive more heat from the sun over
103 the course of a year. Similarly the average precipitation decrease eastward as a result of
104 the influence of longitude: lower longitudes receive less precipitation over the year. Texas
105 bluegrass grows between October and May (growing season), with onset of dormancy often
106 from June to September (dormant season) (Kindiger, 2004). Flowering occurs in May and
107 the species is wind pollinated (Hitchcock, 1971). [The male heads are smooth, while those
108 of the female appear fuzzy.](#)

109 Common garden experiment

110 We set up a common garden experiment throughout and beyond the range of Texas bluegrass
111 to enable study of sex-specific demographic responses to climate and the implications for range
112 shifts. The novelty of this study lies in the fact that we use a precise climate variable to build
113 a mechanistic model to forecast the response of species to climate change. Details of the exper-
114 imental design are provided in Miller and Compagnoni (2022b); we provide a brief overview
115 here. The common experiment was installed at 14 sites across a climatic gradient (Fig.1. At

116 each site, we established 14 blocks. For each block we planted three female and three male indi-
117 viduals that were clonally propagated from eight natural source populations of Texas bluegrass.
118 The experiment was established in November 2013 and was census annually through 2016, pro-
119 viding both spatial and inter-annual variation in climate. Each May (2014-2016), we collected
120 individual demographic data including survival (alive or dead), growth (number of tillers),
121 flowering status (reproductive or vegetative), and fertility (number of panicles, conditional on
122 flowering). For the analyses that follow, we focus on the 2014-15 and 2015-16 transitions years.

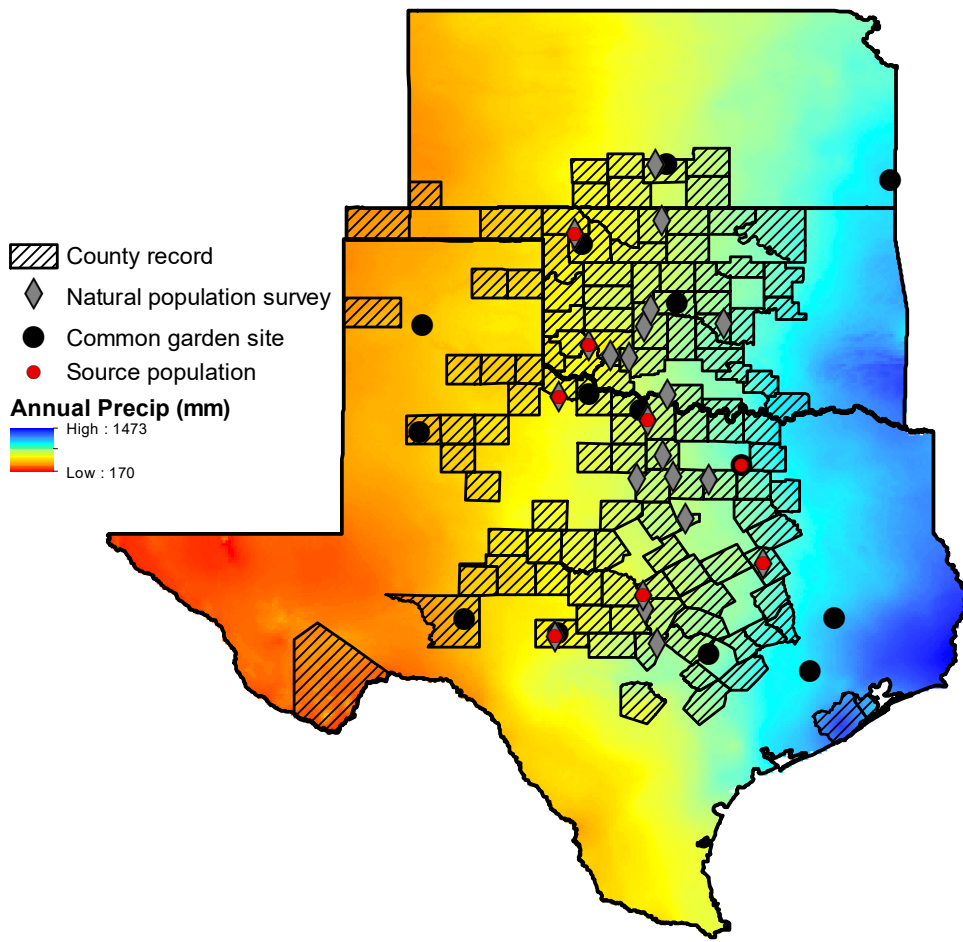


Figure 1: XXX

123 Climatic data collection

124 We downloaded monthly temperature and precipitation from Chelsa to describe observed
125 climate conditions during our study period (Karger et al., 2017). These climate data were used
126 as covariates in vital rate regressions, which allowed us to forecast and back-cast demographic

127 responses to climate change based on observations across the common garden experiment.
128 We aligned the climatic years to match demographic transition years (**May 1 – April 30**)²
129 rather than calendar years. Based on the natural history of this summer-dormant cool-season
130 species, we divided each transition year into growing and dormant seasons. We define June
131 through September as the dormant season and the rest of the year as the growing season.
132 Across years and sites, the experiment included substantial variation in growing and dormant
133 season temperature and precipitation (Supporting Information S-1, S-2).

134 To back-cast and forecast changes in climate, we downloaded projection data for three
135 30-year periods: past (1901-1930), current (1990-2019) and future (2070-2100). Data for these
136 climatic periods were downloaded from four general circulation models (GCMs) selected
137 from the Coupled Model Intercomparison Project Phase 5 (CMIP5). The GCMs are MIROC5,
138 ACCESS1-3, CESM1-BGC, CMCC-CM and were downloaded from chelsa (Sanderson
139 et al., 2015). We evaluated future climate projections from two scenarios of representative
140 concentration pathways (RCPs): RCP4.5, an intermediate-to-pessimistic scenario assuming
141 a radiative forcing to amount to 4.5 Wm^{-2} by 2100, and RCP8.5, a pessimistic emission
142 scenario which project a radiative forcing to amount to 8.5 Wm^{-2} by 2100 (Schwalm et al.,
143 2020; Thomson et al., 2011).

144 Sex ratio experiment

145 We conducted a sex-ratio experiment on a site close (1 km) to a natural population of the
146 focal species at the center of the range to estimate the effect of sex-ratio variation on female
147 reproductive success. Details of the experiment are provided in Compagnoni et al. (2017) and
148 Miller and Compagnoni (2022b). In short, we established 124 experimental populations on
149 plots measuring $0.4 \times 0.4\text{m}$ and separated by at least 15m from each other at that site. We chose
150 15m because our pilot data show that more than 90% of wind pollination occurred within 13m.
151 We varied population density (1-48 plants/plot) and sex ratio (0%-100% female) across the ex-
152 perimental populations, and we replicated 34 combinations of density-sex ratios. We collected
153 the number of panicles from a subset of females in each plot and collected the number of
154 seeds in each panicle. Since the number of panicles (proxy of reproduction effort) does not nec-
155 essarily reflect reproduction success in *Poar arachnifera*, we accessed reproduction success (seed
156 fertilized) using greenhouse-based germination and trazolium-based seed viability assays.

157 We used the sex-ratio to estimate the probability of viability and the germination rate.
158 Seed viability was modeled with a binomial distribution where the probability of viability

²I am not sure if these are actually the right dates.

159 (v) was given by:

160 $v = v_0 * (1 - OSR^\alpha)$ (1)

161 where OSR is the operational sex ratio (proportion of panicles that were female) in the
162 experimental populations. The properties of the above function is supported by our previous
163 work (Compagnoni et al., 2017). Here, seed viability is maximized at v_0 as OSR approaches
164 zero (strongly male-biased) and goes to zero as OSR approaches 1 (strongly female-biased).
165 Parameter α controls how viability declines with increasing female bias.

166 We used a binomial distribution to model the germination data from greenhouse trials.
167 Given that germination was conditional on seed viability, the probability of success was given
168 by the product $v * g$, where v is a function of OSR (Eq. 1) and g is assumed to be constant.

169 Sex specific demographic responses to climate

170 We used individual level measurements of survival, growth (number of tillers), flowering, num-
171 ber of panicles to independently develop Bayesian mixed effect models describing how each
172 vital rate varies as a function of sex, size, precipitation of growing and dormant season and tem-
173 perature of of growing and dormant season. We fit vital rate models with second-degree poly-
174 nomial functions for the influence of climate. We included a second-degree polynomial because
175 we expected that climate variables would affect vital rates through a hump-shaped relationship.

176 We centered and standardized all predictors to facilitate model convergence. We included
177 site, source, and block as random effect. All the vital rate models used the same linear and
178 quadratic predictor for the expected value (μ) (Eq. 2). However, we applied a different
179 link function ($f(\mu)$) depending on the distribution the vital rate. We modeled survival and
180 flowering data with a Bernoulli distribution. We modeled the growth (tiller number) with
181 a zero-truncated Poisson inverse Gaussian distribution. Fertility (panicle count) was model
182 as zero-truncated negative binomial.

$$f(\mu) = \beta_0 + \beta_1 size + \beta_2 sex + \beta_3 pptgrow + \beta_4 pptdorm + \beta_5 tempgrow + \beta_6 tempdorm + \beta_7 pptgrow * sex + \beta_8 pptdorm * sex + \beta_9 tempgrow * sex + \beta_{10} tempdorm * sex + \beta_{11} size * sex + \beta_{12} pptgrow * tempgrow + \beta_{13} pptdorm * tempdorm + \beta_{14} pptgrow * tempgrow * sex + \beta_{15} pptdorm * tempdorm * sex + \beta_{16} pptgrow^2 + \beta_{17} pptdorm^2 + \beta_{18} tempgrow^2 + \beta_{19} tempdorm^2 + \beta_{20} pptgrow^2 * sex + \beta_{21} pptdorm^2 * sex + \beta_{22} tempgrow^2 * sex + \beta_{23} tempdorm^2 * sex + \phi + \rho + \nu \quad (2)$$

184 where β_0 is the grand mean intercept, $\beta_1 \dots \beta_{13}$ represent the size and climate dependent slopes.
 185 *size* was on a natural logarithm scale. *pptgrow* is the precipitation of the growing season
 186 (standardized to mean zero and unit variance), *tempgrow* is the temperature of the growing
 187 season (standardized to mean zero and unit variance), *pptdorm* is the precipitation of the
 188 dormant season (standardized to mean zero and unit variance), *tempdorm* is the temperature
 189 of the dormant season (standardized to mean zero and unit variance). The model also
 190 includes normally distributed random effects for block-to-block variation ($\phi \sim N(0, \sigma_{block})$) and
 191 source-to-source variation that is related to the provenence of the seeds used to establish the
 192 common garden ($\rho \sim N(0, \sigma_{source})$), site to site variation ($v \sim N(0, \sigma_{site})$). We fit survival, growth,
 193 flowering models with generic weakly informative priors for coefficients ($\mu = 0, \sigma = 1.5$) and
 194 variances ($\gamma [0.1, 0.1]$). **We fit fertility model with different generic weakly informative priors**
 195 **for coefficients ($\mu = 0, \sigma = 0.15$)**. We ran three chains for 1000 samples for warmup and 4000
 196 for interactions, with a thinning rate of 3. We accessed the quality of the models using trace
 197 plots and predictive check graphs (Piironen and Vehtari, 2017) (Supporting Information S-4).
 198 To understand the effect of climate on vital rates, we got the 95 % credible interval of the
 199 posterior distribution. Then we assumed that there is 95 % probability that the true (unknown)
 200 estimates would lie within that interval, given the evidence provided by the observed data
 201 for each vital rate. All models were fit in Stan (Stan Development Team, 2023).

202 Population growth rate responses to climate

203 To understand the effect of climate on population growth rate, we used the vital rate estimated
 204 earlier to build a matrix projection model (MPM) structured by size (number of tillers),
 205 sex and climate (dormant and growing) as covariate. Let $F_{x,z,t}$ and $M_{x,z,t}$ be the number of
 206 female and male plants of size x in year t present at a location that has z as climate, where
 207 $x \in \{1, 2, \dots, U\}$ and U is the maximum number of tillers a plant can reach (here 95th percentile
 208 of observed maximum size). Let F_t^R and M_t^R be the new recruits, which we assume do not
 209 reproduce in their first year. We assume that the parameters of sex ratio-dependent mating
 210 (Eq. 1) do not vary with climate. For a pre-breeding census, the expected numbers of recruits
 211 in year $t+1$ is given by:

$$212 F_{t+1}^R = \sum_{x=1}^U [p^F(x,z) \cdot c^F(x,z) \cdot d \cdot v(\mathbf{F}_t, \mathbf{M}_t) \cdot m \cdot \rho] F_{x,z,t} \quad (3)$$

$$213 M_{t+1}^R = \sum_{x=1}^U [p^F(x,z) \cdot c^F(x,z) \cdot d \cdot v(\mathbf{F}_t, \mathbf{M}_t) \cdot m \cdot (1-\rho)] F_{x,z,t} \quad (4)$$

214 where p^F and c^F are flowering probability and panicle production for females of size x , d
 215 is the number of seeds per female panicle, v is the probability that a seed is fertilized, m is
 216 the probability that a fertilized seed germinates, and ρ is the primary sex ratio (proportion
 217 of recruits that are female), z is the climate. Seed fertilization depends on the OSR of panicles
 218 (following Eq. 1) which was derived from the $U \times 1$ vectors of population structure \mathbf{F}_t and \mathbf{M}_t :

$$219 \quad v(\mathbf{F}_t, \mathbf{M}_t) = v_0 * \left[1 - \left(\frac{\sum_{x=1}^U p^F(x,z) c^F(x,z) F_{x,z,t}}{\sum_{x=1}^U p^F(x,z) c^F(x,z) F_{x,z,t} + p^M(x,z) c^M(x,z) M_{x,z,t}} \right)^\alpha \right] \quad (5)$$

220 Thus, the dynamics of the size-structured component of the population are given by:

$$221 \quad F_{y,t+1} = [\sigma \cdot g^F(y, x=1, z)] F_t^R + \sum_{x=1}^U [s^F(x, z) \cdot g^F(y, x, z)] F_{x,z,t} \quad (6)$$

$$222 \quad M_{y,t+1} = [\sigma \cdot g^M(y, x=1, z)] M_t^R + \sum_{x=1}^U [s^M(x, z) \cdot g^M(y, x, z)] M_{x,z,t} \quad (7)$$

223 In the two formula above, the first term indicates seedlings that survived their first year and en-
 224 ter the size distribution of established plants. Instead of using *P. arachnifera* survival probability,
 225 we used the seedling survival probability (σ) from demographic studies of the hermaphroditic
 226 congener *Poa autumnalis* in east Texas (T.E.X. Miller and J.A. Rudgers, *unpublished data*), and we
 227 assume this probability was constant across sexes and climatic variables. We did this because
 228 we had little information on the early life cycle transitions of greenhouse-raised transplants.
 229 We also assume that $g(y, x=1)$ is the probability that a surviving seedlings reach size y ,
 230 the expected future size of 1-tiller plants from the transplant experiment. The second term
 231 represents survival and size transition of established plants from the previous year, where
 232 s and g give the probabilities of surviving at size x and growing from sizes x to y , respectively,
 233 and superscripts indicate that these functions may be unique to females (F) and males (M).

234 Since the two-sex MPM is nonlinear (vital rates affect and are affected by population
 235 structure) we estimated the asymptotic geometric growth rate (λ) by numerical simulation,
 236 and repeated this across a range of climate.

237 Identifying the mechanisms of population growth rate sensitivity to climate

238 To identify which aspect of climate is most important for population viability, we use a
 239 "random design" Life Table Response Experiment (LTRE). We used the RandomForest
 240 package to fit a regression model with θ as predictors and λ_c as response (Ellner et al., 2016;
 241 Liaw et al., 2002). The LTRE approximates the variation in λ in response to climate covariates

242 and their interaction (Caswell, 2000; Hernández et al., 2023):

243

$$Var(\lambda_c) \approx \sum_{i=-1}^n \sum_{j=1}^n Cov(\theta_i, \theta_j, \theta_{ij}) + Var(\epsilon) \quad (8)$$

244 where, θ_i , θ_j , θ_{ij} represent respectively the fitted regression slope for the covariate of the
245 dormant season, j the covariate of the growing season and ij the covariate of their interactions.

246 Because LTRE contributions are additive, we summed across vital rates to compare the
247 total contributions of female and male parameters.

248 Impact of climate change on niche and range shifts

249 A species' ecological niche can be defined as the range of resources and conditions (physical
250 and environmental) allowing the species to maintain a viable population ($\lambda \geq 1$). To
251 understand the impact of climate change on species niche shifts, we estimated the probability
252 of population viability being greater than 1, $Pr(\lambda > 1)$ conditional to two environmental
253 axes (Diez et al., 2014). Because the study species is a cool season grass species, we used
254 two environmental axes: (1) temperature and precipitation of the dormant season and (2)
255 temperature and precipitation of the growing season. $Pr(\lambda > 1)$ was calculated using the
256 proportion of the Markov chain Monte Carlo iterations (here, 300) that lead to a $\lambda > 1$.
257 Population viability-environment relationship was mapped onto geographic layers of three
258 state (Texas, Oklahoma and Kansas) to delineate past, current and future potential distribution
259 of the species. To do so, we estimated $Pr(\lambda > 1)$ as a function of all climate covariates for
260 each pixel (1km*1km) across the species range using the posterior distribution.

261 All the analysis were performed in R 4.3.1 (R Core Team, 2023)

262 Results

263 Sex specific demographic response to climate change

264 Most vital rates were strongly climate dependent, but the magnitude of their response
265 differed between sexes suggesting a sex-specific demographic response to climate. Survival
266 and flowering were strongly more dependent on climate than growth (number of tillers) and
267 reproduction (number of panicles) (Fig.2; Supporting Information S-5). In addition, we found
268 opposite patterns in the direction of the effect on seasonal climate on the probability of survival
269 and flowering. The growing season (precipitation) has a negative effect on the probability of
270 survival, number of tillers, and the probability of flowering, whereas the dormant season has

271 a positive effect on these vital rates. Unlike precipitation, temperature had different effects on
272 different vital rates. Temperature of the growing season has a positive effect of the probability
273 of survival, a negative effect of the probability of flowering, and the number of tillers, but no
274 significant effect on the number of panicles. Further, there was a female survival and flowering
275 advantage across both climatic seasons (Figures. 3A-3D, 3I-3L). On the contrary, there was
276 a male panicle advantage across all climatic variables (Figure3M-3P). Counter-intuitively, there
277 was no significant sex growth advantage in all season climatic variables (Figures. 3E-3H).
278 Plant size x sex interaction was significant for all vitals rates (Supporting Information S-5). For
279 survival, flowering and reproduction the interaction between temperature and precipitation
280 of the growing season and dormant season was not significant (Supporting Information S-5).
281 However, for growth the interaction between temperature and precipitation of the growing
282 season and dormant season was significantly higher than zero (Supporting Information S-5).

283 **Population growth rate response to climate change**

284 We estimated the predicted response of population growth rate (population fitness) to
285 seasonal climate gradients using a model assuming a female dominant model and another
286 model using the two sexes. Consistent with the effect of climate on the individual vital
287 rate, we found a strong effect of seasonal climate on population fitness (Fig.3). For both
288 models (female dominant and two sexes), population fitness decreased with an increase of
289 precipitation of growing season. In contrast population fitness increased with precipitation
290 of the dormant season. Furthermore, population fitness was maximized between 23 and 17
291 °C and decreases to zero just beyond 32 °C during the growing season. Similarly population
292 fitness was maximized between 13 and 17 °C and decreases to zero just beyond 20 °C during
293 the growing season. We have also detected a strong effect of the past and future climate
294 on population growth rate. However, for future climate, the magnitude of that effect was
295 different between gas-scenario emissions. A moderate emission gas scenario (RCP4.5) has a
296 no effect on the population growth rate while a high emission scenario (RCP8.5) has a strong
297 negative effect on the population growth rate. High-emission scenario (RCP8.5) will lead
298 to an alteration of population viability. Under past climate conditions, population growth
299 rate decreased below one for temperature of the growing season and the dormant season.

300 **Climatic niches and range predictions**

301 Across species niche population persistence was maximized at higher temperature during the
302 dormant season (27 to 31) and intermediate temperature during the growing season (11 to
303 20). Our demographically based range predictions broadly captured the known distribution

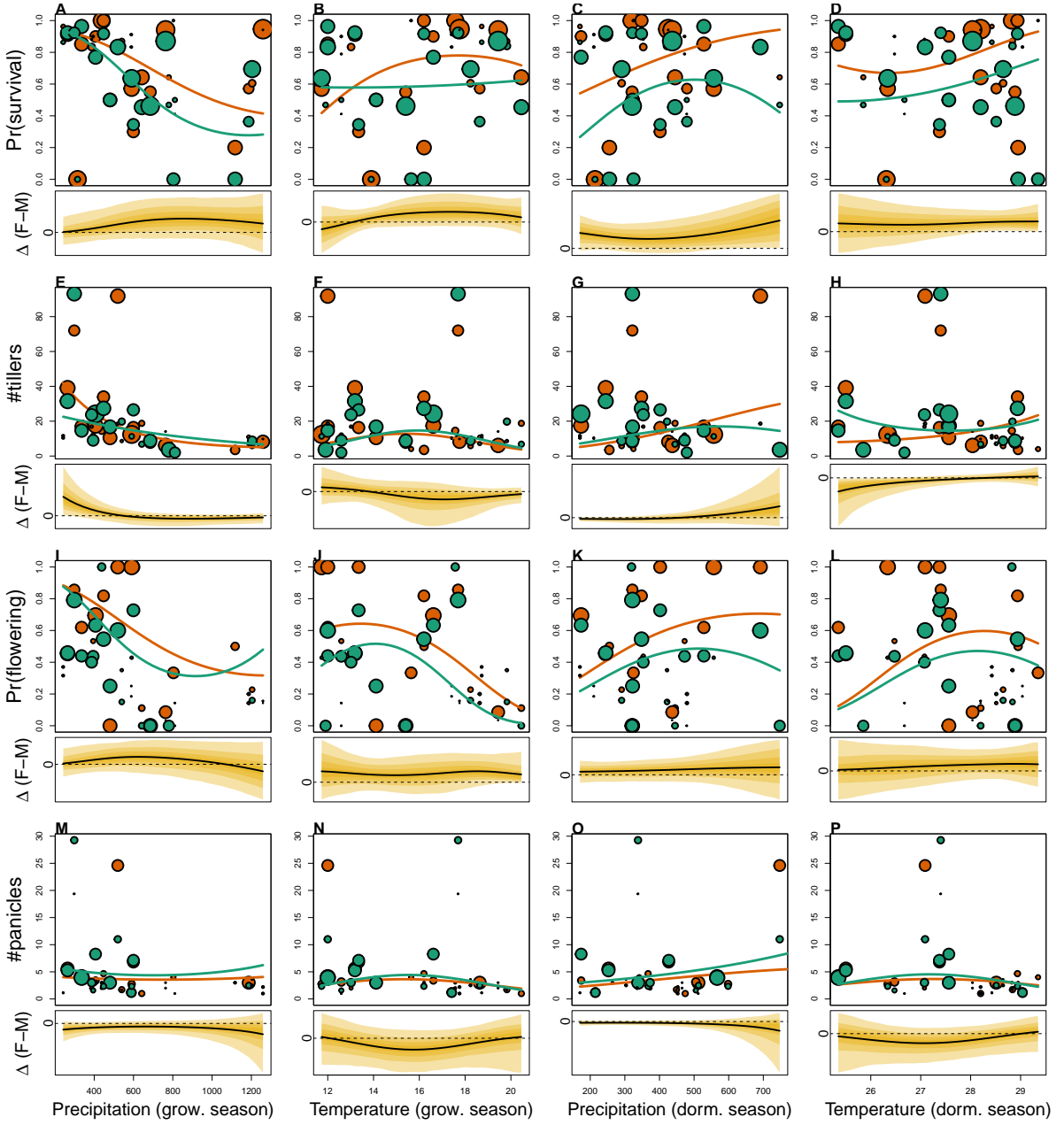


Figure 2: Sex specific demographic response to climate across species range: A–D, inter-annual probability of survival; E–H, inter-annual growth (change in number of tillers); I–L, probability of flowering; M–P, number of panicles produced given flowering. Points show means by site for females (orange) and males (green). Point size is proportional to the sample size of the mean. Lines show fitted statistical models for females (orange) and males (green) based on posterior mean parameter values. Lower panels below each data panel show the posterior distribution of the difference between females and males as a function of climate (positive and negative values indicate female and male advantage, respectively); dashed horizontal line shows zero difference.

304 of the species (Fig. 1). More specifically, the predicted population viable ($\lambda > 1$) matches
 305 the presence and absence of the species. Furthermore, viable populations of *P. arichnifera*

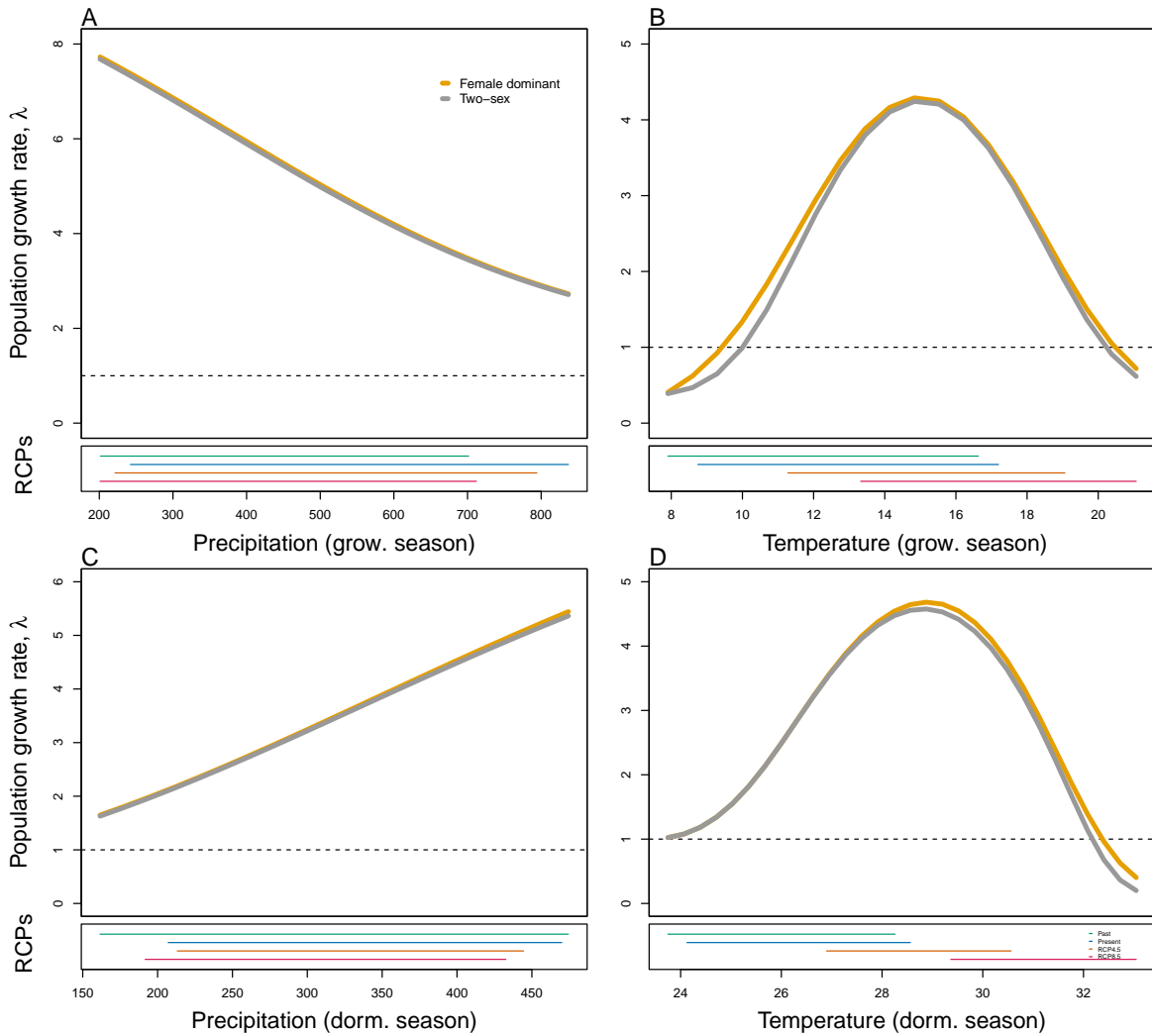


Figure 3: Population growth rate (λ) as a function of climate (past climate, present and predicted future climates). For future climate, we show a Representation Concentration Pathways 4.5 and 8.5. Values of (λ) are derived from the mean climate variables across 4 GCMs. The solid bold curve shows prediction by the two-sex matrix projection model that incorporates sex-specific demographic responses to climate with sex ratio dependent seed fertilization. The bold dashed curve represents the prediction by the female dominant matrix projection model. The dashed horizontal line indicates the limit of population viability ($\lambda = 1$)

were only predicted at the center of the range for current climatic conditions (Fig1). Future and past projections of climate change showed a north-west range shift compared to current distributions. Although *P. archinifera* was predicted to have suitable habitat in the center of the range under the current climate, future warming is predicted to reduce much of the suitable habitat in the southern part (Figure).

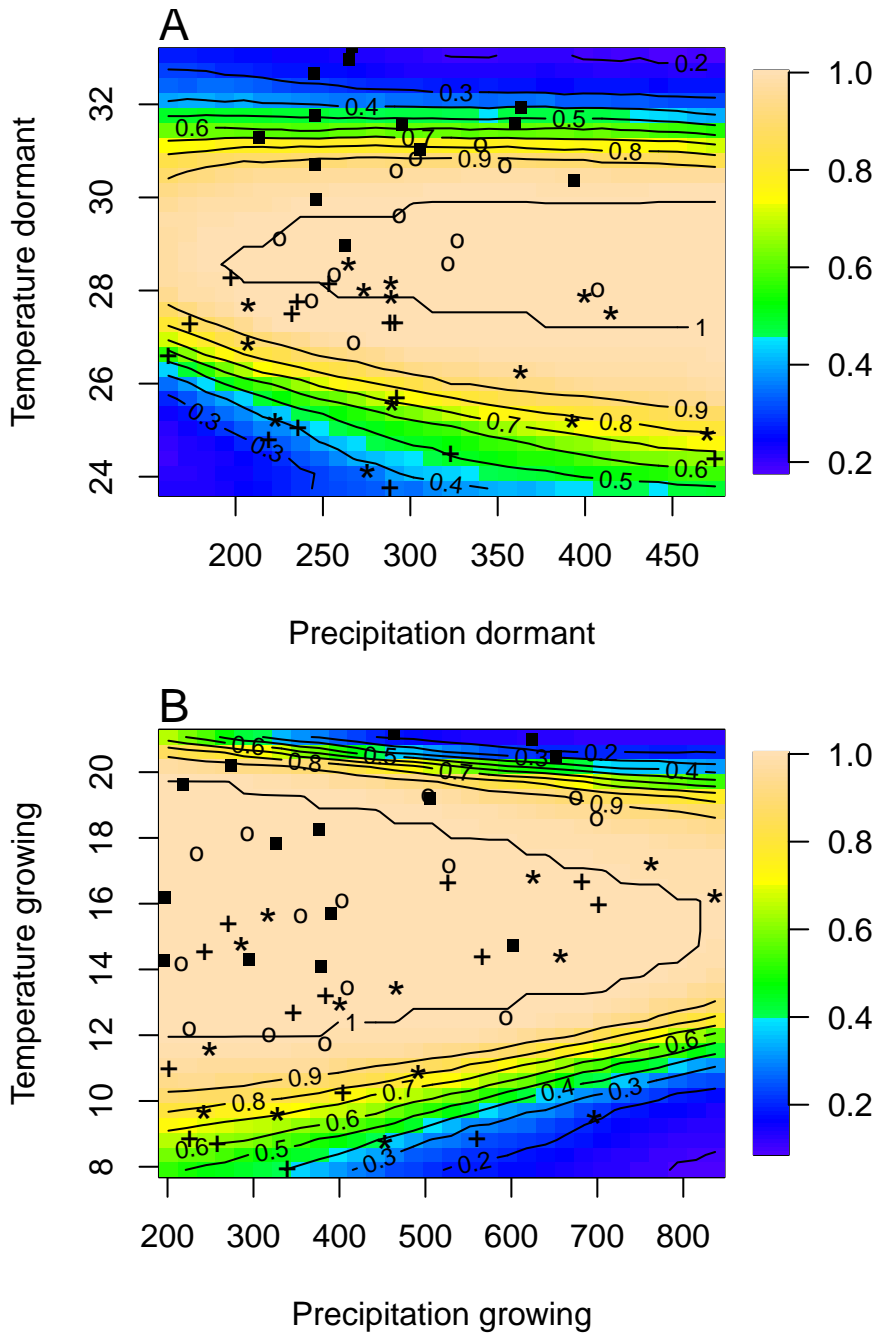


Figure 4: Predicted niche shift for past, present and future climate conditions based on $\text{Pr} (\lambda \geq 1)$. Niche of dormant season (A), Niche of growing season (B). Contours show predicted probabilities of self-sustaining populations $\text{Pr} (\lambda \geq 1)$ conditional on precipitation and temperature of the dormant and growing season

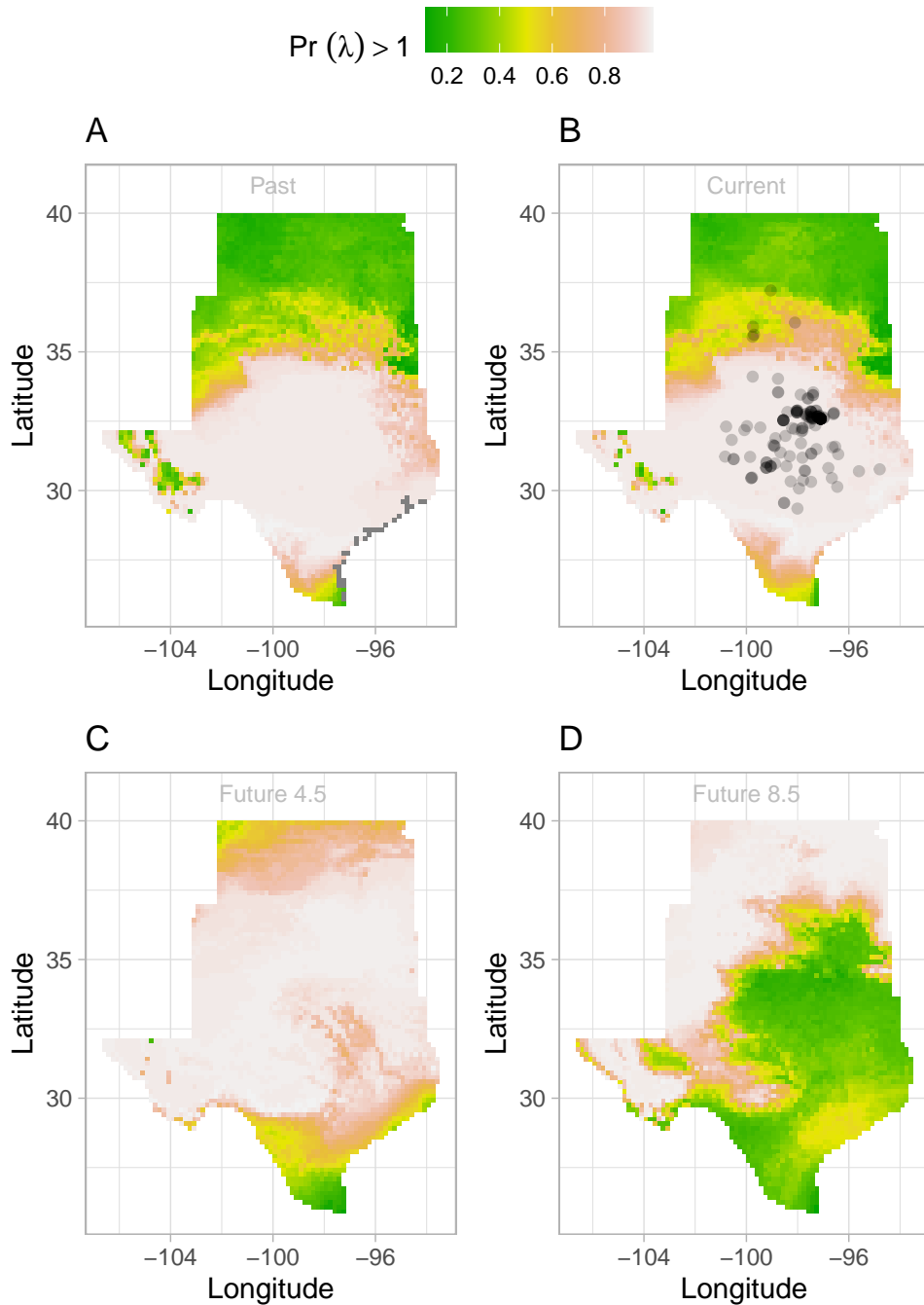


Figure 5: Past (A), Current (B), Future (2070–20100) (C and D) predicted range shift based on population growth rate. Future projections were based on the average population growth rate in four GCMs. The black circles on panel B indicate all known presence points collected from GBIF from 1990 to 2019, which corresponds to the current condition in our prediction. The occurrences of GBIFs are distributed inwith higher population fitness habitat ($\lambda > 1$), confirming that our study approach can reasonably predict range shifts.

311 **Discussion**

312 **References**

- 313 Bertrand, R., Lenoir, J., Piedallu, C., Riofrío-Dillon, G., De Ruffray, P., Vidal, C., Pierrat, J.-C.,
314 and Gégout, J.-C. (2011). Changes in plant community composition lag behind climate
315 warming in lowland forests. *Nature*, 479(7374):517–520.
- 316 Bürli, S., Pannell, J. R., and Tonnabel, J. (2022). Environmental variation in sex ratios and
317 sexual dimorphism in three wind-pollinated dioecious plant species. *Oikos*, 2022(6):e08651.
- 318 Caswell, H. (1989). Analysis of life table response experiments i. decomposition of effects
319 on population growth rate. *Ecological Modelling*, 46(3-4):221–237.
- 320 Caswell, H. (2000). *Matrix population models*, volume 1. Sinauer Sunderland, MA.
- 321 Compagnoni, A., Steigman, K., and Miller, T. E. (2017). Can't live with them, can't live
322 without them? balancing mating and competition in two-sex populations. *Proceedings of
323 the Royal Society B: Biological Sciences*, 284(1865):20171999.
- 324 Czachura, K. and Miller, T. E. (2020). Demographic back-casting reveals that subtle
325 dimensions of climate change have strong effects on population viability. *Journal of Ecology*,
326 108(6):2557–2570.
- 327 Dahlgren, J. P., Bengtsson, K., and Ehrlén, J. (2016). The demography of climate-driven and
328 density-regulated population dynamics in a perennial plant. *Ecology*, 97(4):899–907.
- 329 Davis, M. B. and Shaw, R. G. (2001). Range shifts and adaptive responses to quaternary
330 climate change. *Science*, 292(5517):673–679.
- 331 Diez, J. M., Giladi, I., Warren, R., and Pulliam, H. R. (2014). Probabilistic and spatially variable
332 niches inferred from demography. *Journal of ecology*, 102(2):544–554.
- 333 Eberhart-Phillips, L. J., Küpper, C., Miller, T. E., Cruz-López, M., Maher, K. H., Dos Remedios,
334 N., Stoffel, M. A., Hoffman, J. I., Krüger, O., and Székely, T. (2017). Sex-specific early
335 survival drives adult sex ratio bias in snowy plovers and impacts mating system and
336 population growth. *Proceedings of the National Academy of Sciences*, 114(27):E5474–E5481.
- 337 Ellis, R. P., Davison, W., Queirós, A. M., Kroeker, K. J., Calosi, P., Dupont, S., Spicer, J. I.,
338 Wilson, R. W., Widdicombe, S., and Urbina, M. A. (2017). Does sex really matter? explaining
339 intraspecies variation in ocean acidification responses. *Biology letters*, 13(2):20160761.

- 340 Ellner, S. P., Childs, D. Z., Rees, M., et al. (2016). Data-driven modelling of structured
341 populations. *A practical guide to the Integral Projection Model*. Cham: Springer.
- 342 Evans, M. E., Merow, C., Record, S., McMahon, S. M., and Enquist, B. J. (2016). Towards
343 process-based range modeling of many species. *Trends in Ecology & Evolution*, 31(11):860–871.
- 344 Gamelon, M., Grøtan, V., Nilsson, A. L., Engen, S., Hurrell, J. W., Jerstad, K., Phillips, A. S.,
345 Røstad, O. W., Slagsvold, T., Walseng, B., et al. (2017). Interactions between demography
346 and environmental effects are important determinants of population dynamics. *Science
347 Advances*, 3(2):e1602298.
- 348 Gissi, E., Schiebinger, L., Hadly, E. A., Crowder, L. B., Santoleri, R., and Micheli, F. (2023a).
349 Exploring climate-induced sex-based differences in aquatic and terrestrial ecosystems to
350 mitigate biodiversity loss. *nature communications*, 14(1):4787.
- 351 Gissi, E., Schiebinger, L., Santoleri, R., and Micheli, F. (2023b). Sex analysis in marine biological
352 systems: insights and opportunities. *Frontiers in Ecology and the Environment*.
- 353 Hernández, C. M., Ellner, S. P., Adler, P. B., Hooker, G., and Snyder, R. E. (2023). An exact
354 version of life table response experiment analysis, and the r package exactltre. *Methods
355 in Ecology and Evolution*, 14(3):939–951.
- 356 Hitchcock, A. S. (1971). *Manual of the grasses of the United States*, volume 2. Courier Corporation.
- 357 Hultine, K. R., Grady, K. C., Wood, T. E., Shuster, S. M., Stella, J. C., and Whitham, T. G. (2016).
358 Climate change perils for dioecious plant species. *Nature Plants*, 2(8):1–8.
- 359 Iler, A. M., Compagnoni, A., Inouye, D. W., Williams, J. L., CaraDonna, P. J., Anderson, A., and
360 Miller, T. E. (2019). Reproductive losses due to climate change-induced earlier flowering are
361 not the primary threat to plant population viability in a perennial herb. *Journal of Ecology*,
362 107(4):1931–1943.
- 363 Jones, M. H., Macdonald, S. E., and Henry, G. H. (1999). Sex-and habitat-specific responses
364 of a high arctic willow, *salix arctica*, to experimental climate change. *Oikos*, pages 129–138.
- 365 Karger, D. N., Conrad, O., Böhner, J., Kawohl, T., Kreft, H., Soria-Auza, R. W., Zimmermann,
366 N. E., Linder, H. P., and Kessler, M. (2017). Climatologies at high resolution for the earth's
367 land surface areas. *Scientific data*, 4(1):1–20.
- 368 Kindiger, B. (2004). Interspecific hybrids of *poa arachnifera* × *poa secunda*. *Journal of New
369 Seeds*, 6(1):1–26.

- 370 Lee-Yaw, J. A., Kharouba, H. M., Bontrager, M., Mahony, C., Csergő, A. M., Noreen, A. M.,
371 Li, Q., Schuster, R., and Angert, A. L. (2016). A synthesis of transplant experiments and
372 ecological niche models suggests that range limits are often niche limits. *Ecology letters*,
373 19(6):710–722.
- 374 Leicht-Young, S. A., Silander, J. A., and Latimer, A. M. (2007). Comparative performance of
375 invasive and native celastrus species across environmental gradients. *Oecologia*, 154:273–282.
- 376 Liaw, A., Wiener, M., et al. (2002). Classification and regression by randomforest. *R news*,
377 2(3):18–22.
- 378 Louthan, A. M., Keighron, M., Kiekebusch, E., Cayton, H., Terando, A., and Morris, W. F.
379 (2022). Climate change weakens the impact of disturbance interval on the growth rate of
380 natural populations of venus flytrap. *Ecological Monographs*, 92(4):e1528.
- 381 Merow, C., Bois, S. T., Allen, J. M., Xie, Y., and Silander Jr, J. A. (2017). Climate change both
382 facilitates and inhibits invasive plant ranges in new england. *Proceedings of the National
383 Academy of Sciences*, 114(16):E3276–E3284.
- 384 Miller, T. and Compagnoni, A. (2022a). Data from: Two-sex demography, sexual niche
385 differentiation, and the geographic range limits of texas bluegrass (*Poa arachnifera*). *American
386 Naturalist, Dryad Digital Repository*. <https://doi.org/10.5061/dryad.kkwh70s5x>.
- 387 Miller, T. E. and Compagnoni, A. (2022b). Two-sex demography, sexual niche differentiation,
388 and the geographic range limits of texas bluegrass (*poa arachnifera*). *The American
389 Naturalist*, 200(1):17–31.
- 390 Morrison, C. A., Robinson, R. A., Clark, J. A., and Gill, J. A. (2016). Causes and consequences
391 of spatial variation in sex ratios in a declining bird species. *Journal of Animal Ecology*,
392 85(5):1298–1306.
- 393 Morrison, S. F. and Hik, D. S. (2007). Demographic analysis of a declining pika *ochotona
394 collaris* population: linking survival to broad-scale climate patterns via spring snowmelt
395 patterns. *Journal of Animal ecology*, pages 899–907.
- 396 O’Connell, R. D., Doak, D. F., Horvitz, C. C., Pascarella, J. B., and Morris, W. F. (2024). Nonlinear
397 life table response experiment analysis: Decomposing nonlinear and nonadditive population
398 growth responses to changes in environmental drivers. *Ecology Letters*, 27(3):e14417.
- 399 Pease, C. M., Lande, R., and Bull, J. (1989). A model of population growth, dispersal and
400 evolution in a changing environment. *Ecology*, 70(6):1657–1664.

- 401 Petry, W. K., Soule, J. D., Iler, A. M., Chicas-Mosier, A., Inouye, D. W., Miller, T. E., and
402 Mooney, K. A. (2016). Sex-specific responses to climate change in plants alter population
403 sex ratio and performance. *Science*, 353(6294):69–71.
- 404 Piironen, J. and Vehtari, A. (2017). Comparison of bayesian predictive methods for model
405 selection. *Statistics and Computing*, 27:711–735.
- 406 Pottier, P., Burke, S., Drobniak, S. M., Lagisz, M., and Nakagawa, S. (2021). Sexual (in) equality?
407 a meta-analysis of sex differences in thermal acclimation capacity across ectotherms.
408 *Functional Ecology*, 35(12):2663–2678.
- 409 R Core Team (2023). *R: A Language and Environment for Statistical Computing*. R Foundation
410 for Statistical Computing, Vienna, Austria.
- 411 Sanderson, B. M., Knutti, R., and Caldwell, P. (2015). A representative democracy to reduce
412 interdependency in a multimodel ensemble. *Journal of Climate*, 28(13):5171–5194.
- 413 Sasaki, M., Hedberg, S., Richardson, K., and Dam, H. G. (2019). Complex interactions
414 between local adaptation, phenotypic plasticity and sex affect vulnerability to warming
415 in a widespread marine copepod. *Royal Society open science*, 6(3):182115.
- 416 Schwalm, C. R., Glendon, S., and Duffy, P. B. (2020). Rcp8. 5 tracks cumulative co2 emissions.
417 *Proceedings of the National Academy of Sciences*, 117(33):19656–19657.
- 418 Schwinning, S., Lortie, C. J., Esque, T. C., and DeFalco, L. A. (2022). What common-garden
419 experiments tell us about climate responses in plants.
- 420 Sexton, J. P., McIntyre, P. J., Angert, A. L., and Rice, K. J. (2009). Evolution and ecology of
421 species range limits. *Annu. Rev. Ecol. Evol. Syst.*, 40:415–436.
- 422 Smith, M. D., Wilkins, K. D., Holdrege, M. C., Wilfahrt, P., Collins, S. L., Knapp, A. K., Sala,
423 O. E., Dukes, J. S., Phillips, R. P., Yahdjian, L., et al. (2024). Extreme drought impacts have
424 been underestimated in grasslands and shrublands globally. *Proceedings of the National
425 Academy of Sciences*, 121(4):e2309881120.
- 426 Stan Development Team (2023). RStan: the R interface to Stan. R package version 2.21.8.
- 427 Thomson, A. M., Calvin, K. V., Smith, S. J., Kyle, G. P., Volke, A., Patel, P., Delgado-Arias,
428 S., Bond-Lamberty, B., Wise, M. A., Clarke, L. E., et al. (2011). Rcp4. 5: a pathway for
429 stabilization of radiative forcing by 2100. *Climatic change*, 109:77–94.

- ⁴³⁰ Tognetti, R. (2012). Adaptation to climate change of dioecious plants: does gender balance
⁴³¹ matter? *Tree Physiology*, 32(11):1321–1324.
- ⁴³² Welbergen, J. A., Klose, S. M., Markus, N., and Eby, P. (2008). Climate change and the
⁴³³ effects of temperature extremes on australian flying-foxes. *Proceedings of the Royal Society
B: Biological Sciences*, 275(1633):419–425.
- ⁴³⁵ Zhao, H., Li, Y., Zhang, X., Korpelainen, H., and Li, C. (2012). Sex-related and stage-dependent
⁴³⁶ source-to-sink transition in *populus cathayana* grown at elevated co₂ and elevated
⁴³⁷ temperature. *Tree Physiology*, 32(11):1325–1338.

Supporting Information

438 S.1 XX

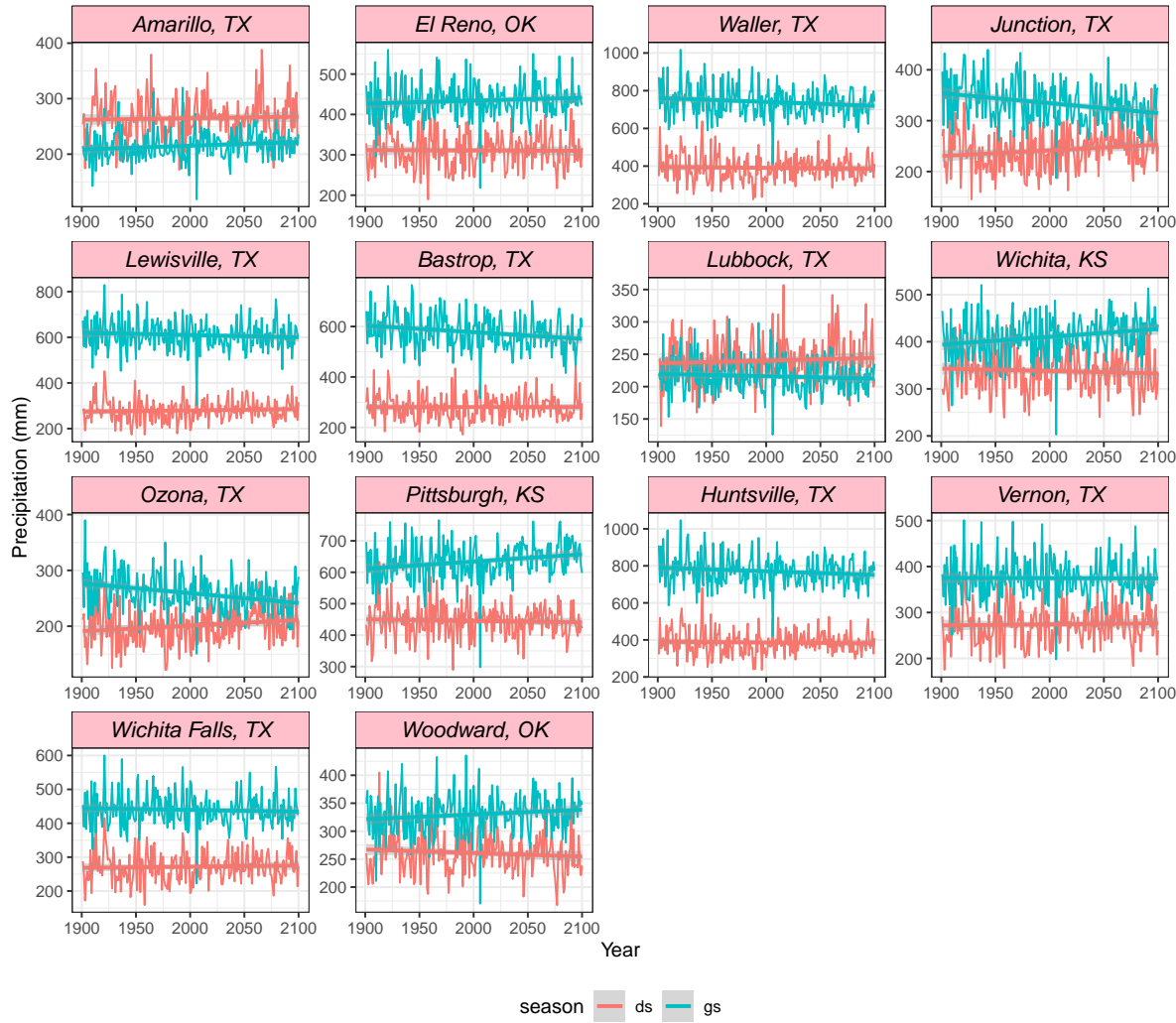


Figure S-1: Precipitation variation across the study sites from 1990 to 2100

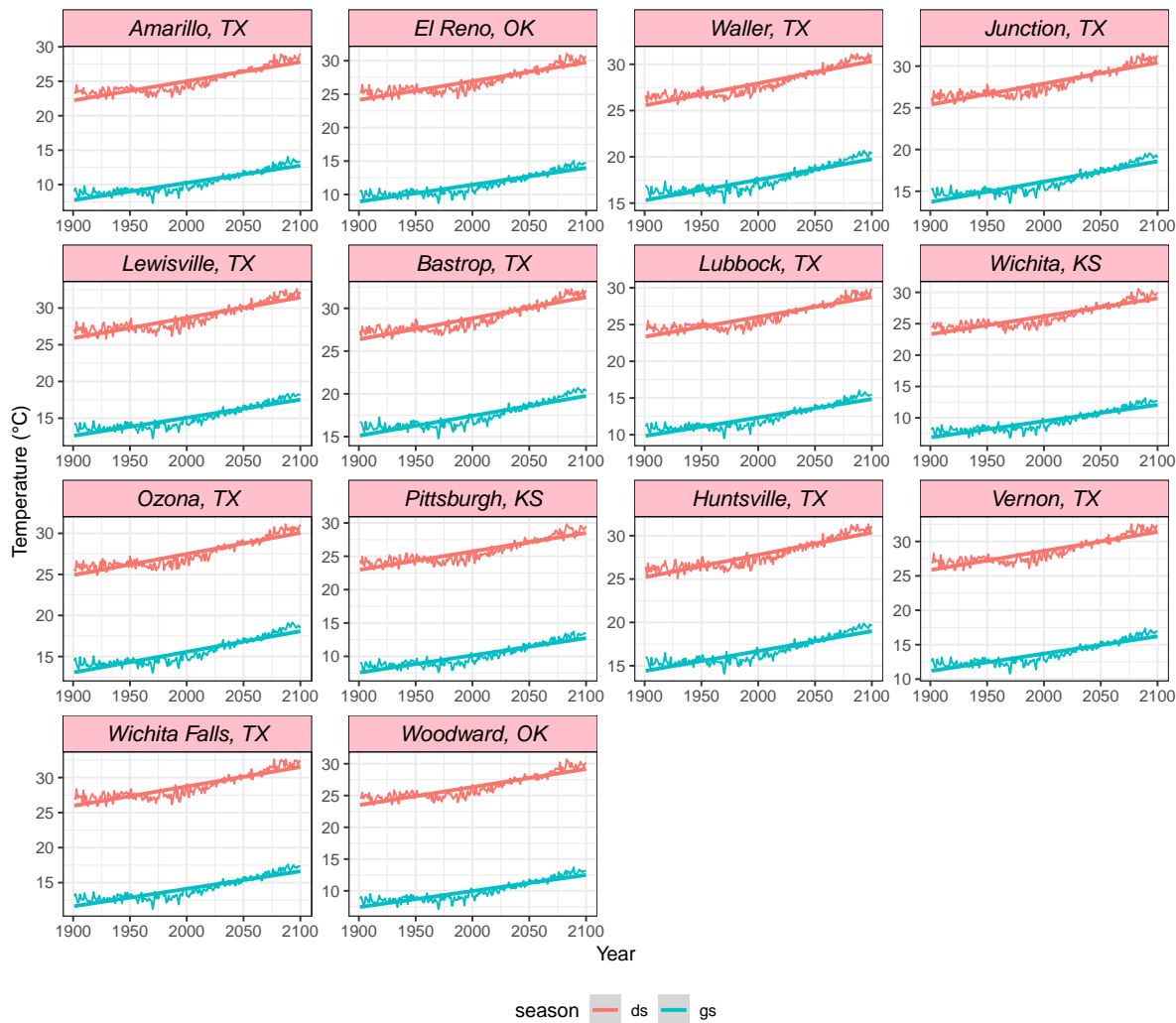


Figure S-2: Temperature variation across the study sites from 1990 to 2100

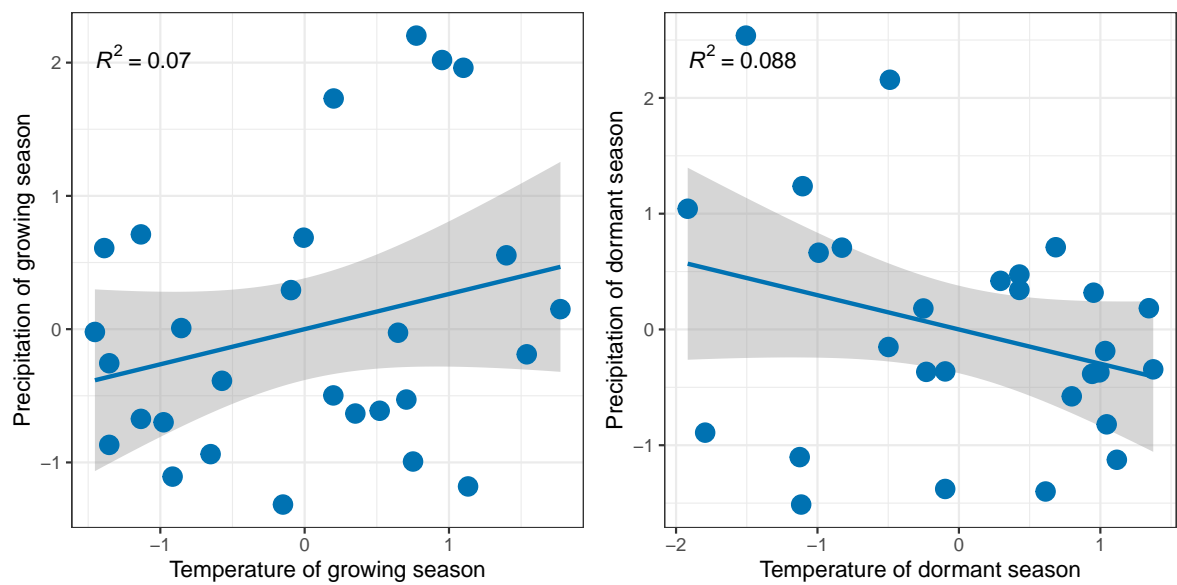


Figure S-3: Relation between precipitation and temperature for each season (growing and dormant). R^2 indicates the value of proportion of explained variance between the temperature and precipitation

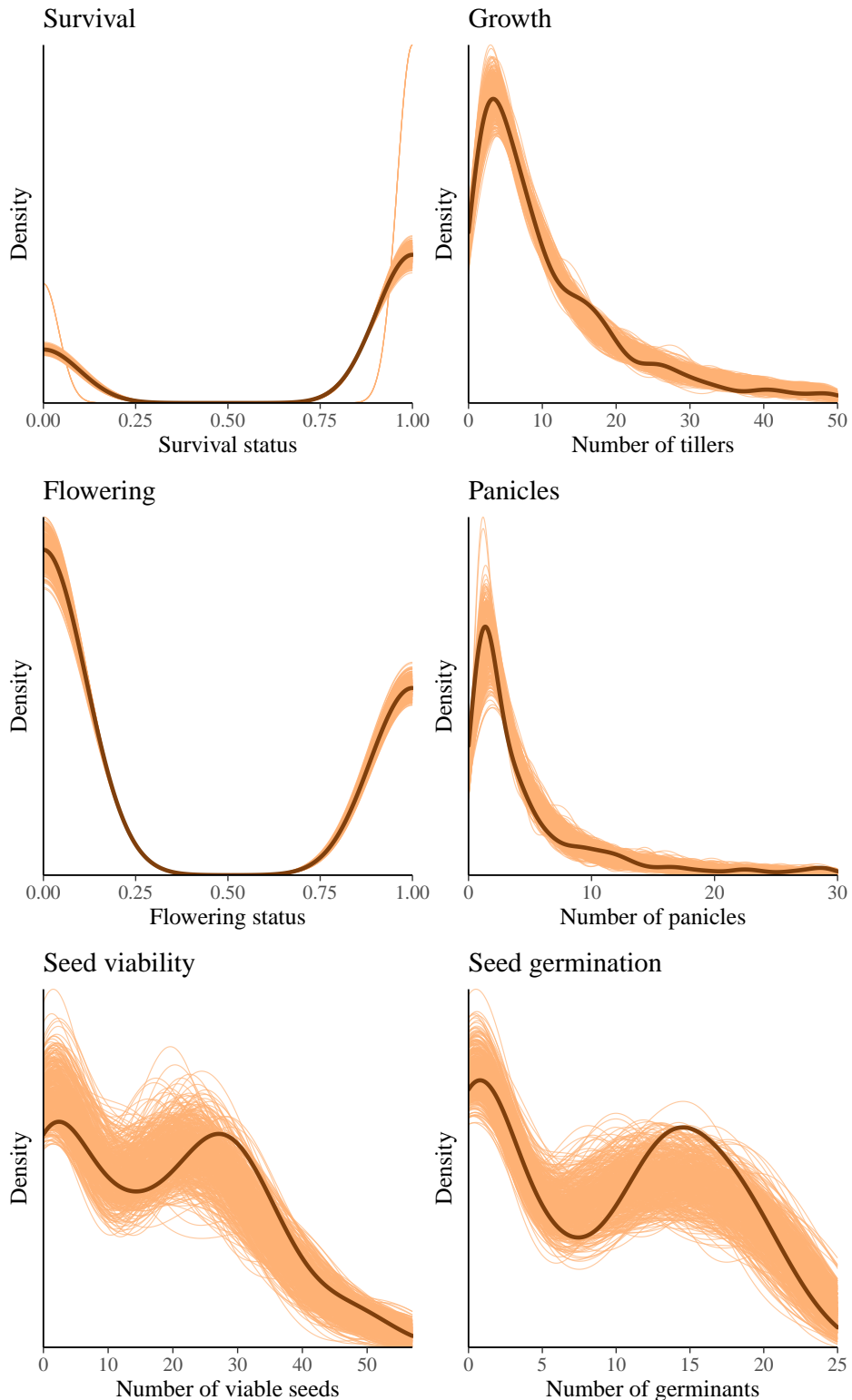


Figure S-4: Consistency between real data and simulated values suggests that the fitted model accurately describes the data. Graph shows density curves for the observed data (light blue) along with the simulated values (dark blue). The first column shows the linear models and the second column shows the 2 degree polynomial models.

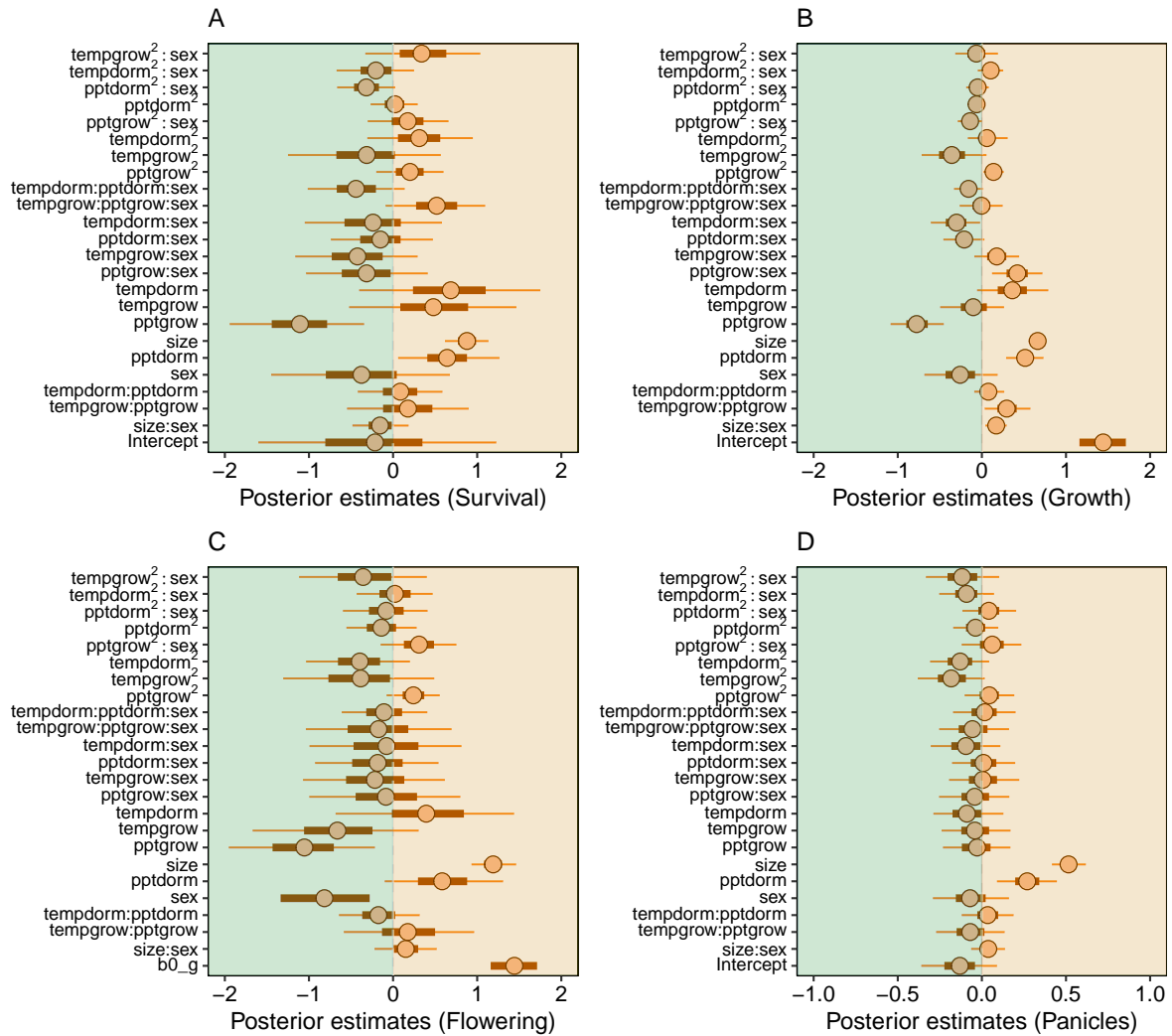


Figure S-5: Mean parameter values and 95% credible intervals for all vital rates.

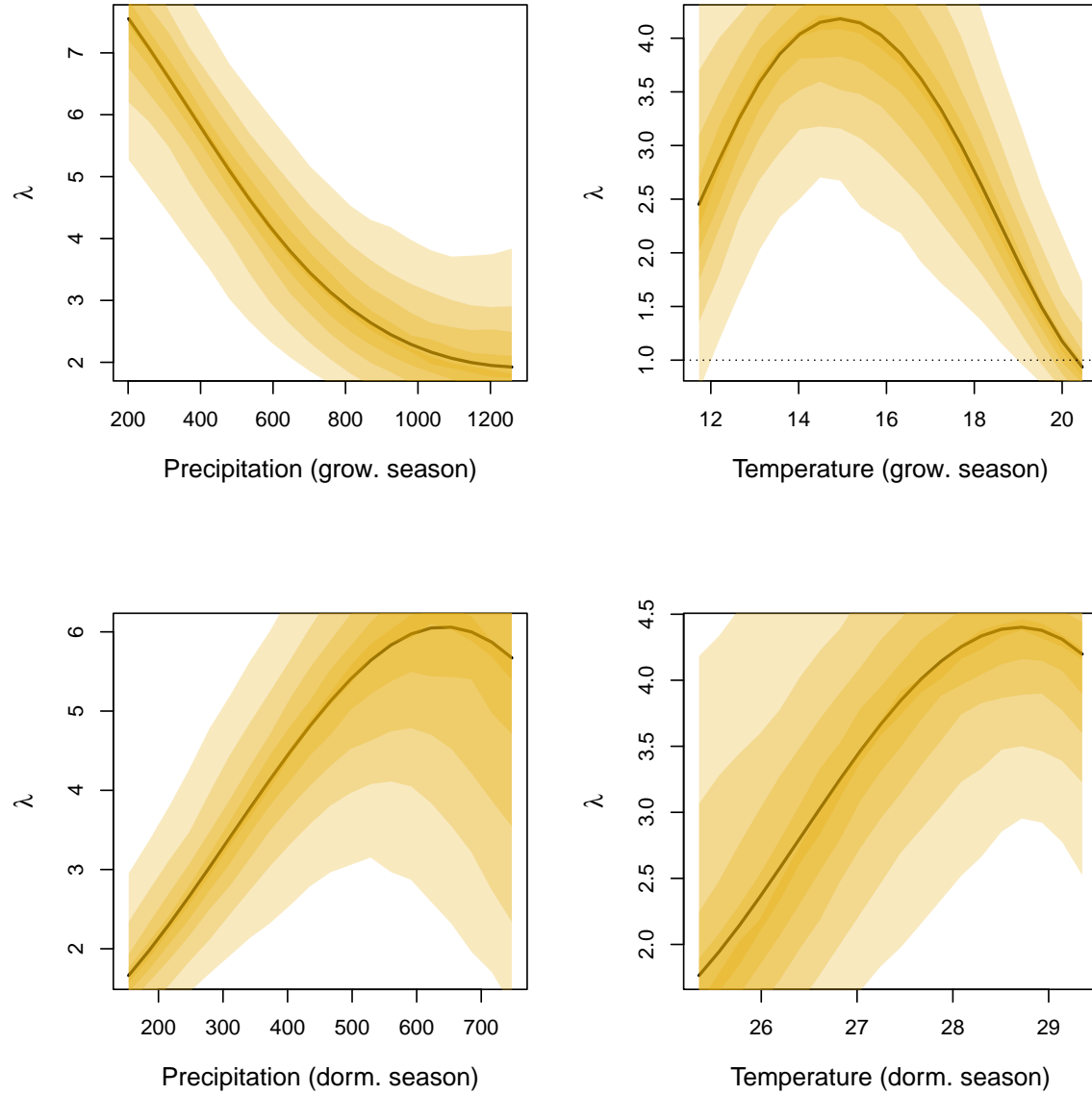


Figure S-6: Population growth rate (λ) as a function of seasonal climate (2016-2017), predicted by the two-sex matrix projection model that incorporates sex-specific demographic responses to climate with sex ratio-dependent seed fertilization. We show the mean posterior distribution of λ in solid lines, and the 5, 25, 50, 75, and 95% percentiles of parameter uncertainty in shaded gold color. The dashed horizontal line indicates the limit of population viability ($\lambda = 1$)

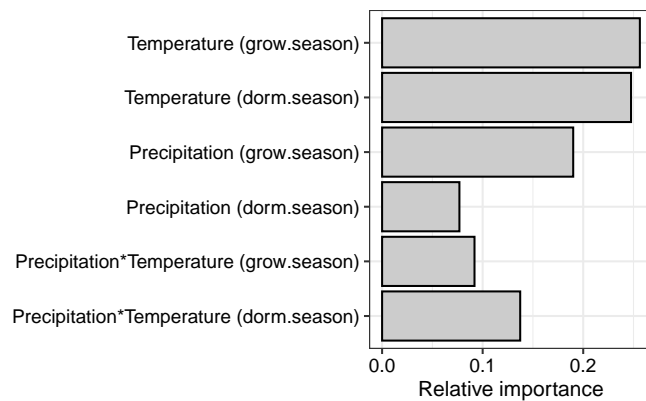


Figure S-7: XXX